



Journal of Applied Sciences

ISSN 1812-5654

science
alert

ANSI*net*
an open access publisher
<http://ansinet.com>

Lattice Instability of 2H-TaS₂

S. Antony Raj and N. Lawrence

Department of Physics, St. Joseph's College, Tiruchirappalli, 620 002, India

Abstract: At low temperatures, the layered compound such as 2H-TaS₂ are commonly found to exhibit super-lattice which is commensurate with the primitive lattice. Transition from normal to In-Commensurate Charge Density Wave (ICCDW) is driven by the coupling of strong electron-phonon and favored by the particular form of the Fermi surface of these systems. On set, temperature of ICCDW influences the electrical as well as the thermal properties of this system. In this study, Born-von Karman is used in calculating the phonon frequency distribution curves of 2H-TaS₂ in ICCDW and normal phases. In this phase, a folding technique has been used for the estimation and the distributions of the phonon and the thermal properties have been evaluated and reported for both the phases and the results are compared with the existing literature results.

Key words: Super-lattice, ICCDW, Born-von karman formalism, phonon distributions

INTRODUCTION

Charge Density Wave (CDW) is a dramatic phenomenon where coupling of the electron-phonon works with the 'Fermi surface nesting' results in the spatial modulation of the crystalline lattice and conduction-electron density. The formation of CDW's in one-dimensional systems was first suggested by Peierls (1995) and Frohlich (1954). However, at low temperatures the lattice will not be stable. The instability is due to the periodic potential presence which will break the distribution of Fermi surface which induces charge density wave. The 2H-TaS₂ has hexagonal structure and has interesting phase change behaviour. It is in the ICCDW phase below 75 K and in normal phase above this transition temperature (Sugai, 1985). In ICCDW phase, it has unit cell of size $3a_0 \times 3a_0 \times c_0$, where a_0 and c_0 are the lattice constants.

Many experimental studies (Brouet *et al.*, 2004; Shin *et al.*, 2005; Lavagnini *et al.*, 2008) are available to study the characteristics of CDW system such as 2H-TaS₂. The available theoretical model describes the electron-phonon interaction in the CDW formation. But a few experimental studies (Harper *et al.*, 1977; Sugai *et al.*, 1981; Wilson *et al.*, 2001) are available to investigate the variation of thermal properties with temperature in the context of CDW. Hence, it has been planned to investigate the dynamical behaviour of the lattice and the contribution of phonons towards the thermal properties of this system. In this study, phonon frequency distribution, thermal properties includes Debye Waller factor and specific heat capacity are calculated and in

normal and ICCDW phases the thermal conductivity for 2H-TaS₂ are reported (Balaguru *et al.*, 2002).

CALCULATION PROCEDURE

The space group of 2H-TaS₂ is D_{6h}^4 . It has two layers and six atoms per unit cell namely two Ta atoms (Type 1 and 2) and four S atoms (Type 3, 4, 5 and 6). In Cartesian frame, the basic vectors of unit are given by:

$$a_1 = \left(\frac{1}{2}\right)a(\sqrt{3}\hat{i} - \hat{j})$$
$$a_2 = a\hat{j}$$

and:

$$a_3 = c\hat{k}$$

The unit vectors of the reciprocal Lattice are given by:

$$b_1 = \left(\frac{2}{\sqrt{3}a}\right)\hat{i}$$
$$b_2 = \left(\frac{1}{\sqrt{3}a}\right)\hat{i} + \left(\frac{1}{a}\right)\hat{j}$$

and:

$$b_3 = \left(\frac{1}{c}\right)\hat{k}$$

In lower layer, the Ta₁, two S₃ and S₄ are denoted by:

$$(0, 0, -\frac{c}{4}), (-\frac{a}{3}, -2\frac{a}{3}, uc - \frac{c}{2})$$

and:

$$(\frac{-a}{3}, \frac{-2a}{3}, -uc)$$

respectively. In upper layer, the coordinates of Ta₂, two S₅ and S₆ are:

$$(0, 0, \frac{c}{4}), (\frac{a}{3}, \frac{2a}{3}, uc)$$

and:

$$(\frac{a}{3}, \frac{2a}{3}, -uc + \frac{c}{2})$$

respectively, where a, c and u are lattice parameters having values 3.35 Å, 12.10 Å and 0.118, respectively.

Born-Von Karman model has been used to illustrate the force constant tensor of the Ta-S interaction. The lower layer force constant is represented by:

$$\begin{bmatrix} A & B & -C \\ B & D & -E \\ -C & -E & F_1 \end{bmatrix}$$

and the upper layer is represented by six parameters:

$$\begin{bmatrix} A & B & C \\ B & D & E \\ C & E & F \end{bmatrix}$$

using the symmetry property the force constant tensor can be created for the remaining S neighbors. For the S-S interactions of same type, the force constant parameters are given by A₅ and B₅. A₃ and B₃ denotes the force constant parameter for Ta-Ta interactions of same type and A₄ and B₄ represents the Ta-Ta interactions of different type. Pawley's potential (Rinaldi and Pawley, 1975) will fix the values for these parameters which will be in units of 10⁴ dyne cm⁻¹ as:

$$\begin{array}{lll} A_1 = 0.9943 & B_1 = -5.6424 & C_1 = 0.7362 \\ D_1 = -3.9245 & E_1 = -5.8750 & F_1 = 0.3312 \\ A_2 = -1.2317 & B_2 = 0.0722 & A_3 = -0.0768 \\ B_3 = 0.0234 & A_4 = -0.9326 & B_4 = 0.0623 \\ A_5 = 1.3260 & B_5 = -0.3528 & \end{array}$$

The dynamical matrix represents Hermitian matrix of (18×18) (as shown in Appendix 1) will be diffused into

(36×36) matrix. The diagonalization of this real symmetric matrix results in phonon frequencies and polarization vectors.

In normal phase, by uniformly dividing the Brillouin zone, phonon frequencies for a set of 84 wave-vector points (Di Salvo *et al.*, 1976). In ICCDW phase, to calculate phonon frequencies for a set of 336 wave vector points a folding technique has been used. Using values and vectors, Debye Waller factor and thermal conductivity of 2H-TaS₂ t in the variation of specific heat capacity with reference to temperature in both the phases are reported by following the previous study (Berman, 1976; Nunez-Regueiro *et al.*, 1985).

RESULTS AND DISCUSSION

Figure 1 represents phonon frequency distribution curves. The blank circled 'C' line and the black circled 'B' curve represent the normal phase and ICCDW phase, respectively. From the figures, most of the frequency modes are distributed in low frequency of the ICCDW as compared to normal one which results in less electron scattering by phonons in the ICCDW phase. In addition to the beginning of CDW and because of the less electron phonon scattering, the resistivity is expected to decrease in the ICCDW phase. Hence, the present result supports the superconducting behavior of this material at low temperature as observed by Smith *et al.* (1975).

Figure 2 represents the 0-265 k variation in specific heat. Since, the phase transition occurs at 75 K, in ICCDW phase the frequency distribution data has been used below this transition and in normal phase above the transition phase. From the graph, discontinuity occurs at the transition temperature. At the transition temperature, this discontinuity may be attributed to the change of the

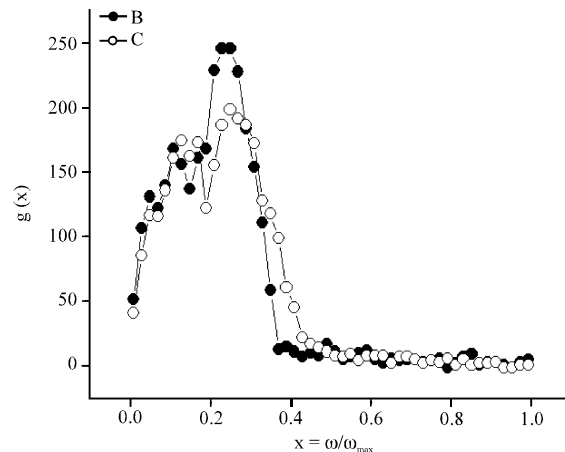


Fig. 1: Phonon frequency distribution

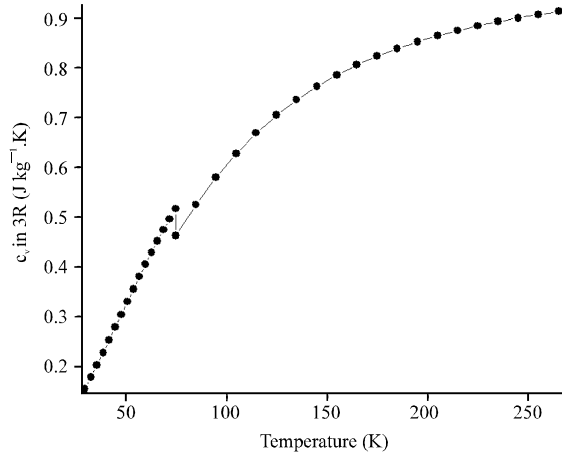


Fig. 2: Specific heat variation with temperature

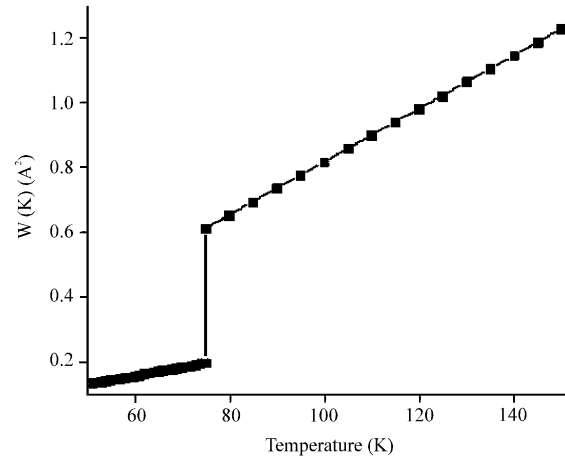


Fig. 4: Debye waller factor of sulfur atoms

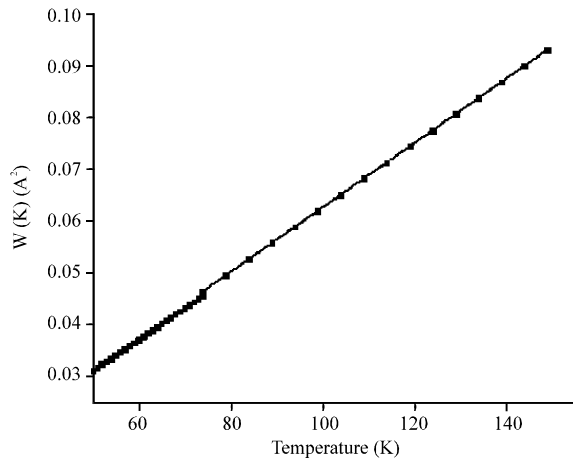


Fig. 3: Debye waller factor of tantalum atoms

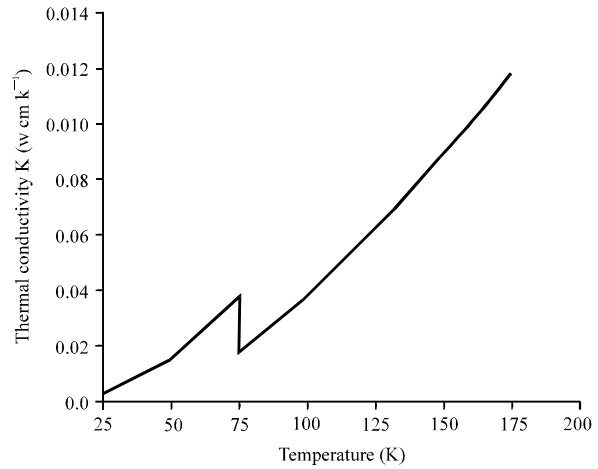


Fig. 5: Thermal conductivity of 2H-TaS₂

distributed phonon frequency. The observed results are comparable with Craven and Meyer (1977).

Using the respective Eigen values and vectors for both the phases, Ta and S Debye Waller factor values at different temperatures have been calculated. The curves for both the types of atoms are shown in Fig. 3 and 4, respectively. At the transition temperature, an anomalous behavior is observed from these curves that may be due to the electron-phonon interaction change in the ICCDW phase and due to the increase in the size of the unit cell. From these figures, Ta atoms are displaced lesser than chalcogen atoms due to the heavier nature of Ta atom and is comparable with the results of Moncton *et al.* (1977).

For the range of 25-175 K, the thermal conductivity and temperature curve are shown in Fig. 5 that shows a discontinuity at 75 K, the transition temperature as expected and also results in a drastic decrease that occurs due to the heavy change in the concentration of electrons

and mainly due to phonon frequency modes in larger number in ICCDW phase. Thus, the lattice vibration forms the contributions to the thermal conductivity and hence, the phonon frequency modes. This curve is similar to the curve observed for 2H-NbSe₂.

CONCLUSION

The phonon frequencies of the normal phase for 2H-TaS₂ have been computed using 84 wave vector points obtained by uniformly dividing the Brillouin zone. For ICCDW phase, they were computed using 336 wave vector points generated using folding technique. The phonon frequency distribution curves have been drawn and using them, the thermal properties such as the specific heat capacity, the Debye Waller factor for both atoms (Ta and S) and the thermal conductivity for both the phases have been computed. The present results are in good agreement with the experimental results.

Appendix 1: From the diagonalization of the dynamical matrix, the phonon frequencies and their polarization vectors can be obtained. Maradudin *et al.* (1971) having elements as follows:

$$\begin{aligned} \begin{pmatrix} 1 & 1 \\ x & x \end{pmatrix} &= A_3 f_1 \\ \begin{pmatrix} 1 & 1 \\ y & y \end{pmatrix} &= A_3 f_1 \\ \begin{pmatrix} 1 & 1 \\ z & z \end{pmatrix} &= B_3 f_1 \\ \begin{pmatrix} 1 & 2 \\ x & x \end{pmatrix} &= A_4 f_2 \\ \begin{pmatrix} 1 & 2 \\ y & y \end{pmatrix} &= A_4 f_2 \\ \begin{pmatrix} 1 & 2 \\ z & z \end{pmatrix} &= B_4 f_2 \\ \begin{pmatrix} 2 & 2 \\ x & x \end{pmatrix} &= A_3 f_3 \\ \begin{pmatrix} 2 & 2 \\ y & y \end{pmatrix} &= A_3 f_3 \\ \begin{pmatrix} 2 & 2 \\ z & z \end{pmatrix} &= B_3 f_3 \\ \begin{pmatrix} 1 & 3 \\ x & x \end{pmatrix} &= A_1 f_{11} + \left(\frac{A_1 + \sqrt{3}B_1 + 3D_1}{4} \right) f_{12} + \left(\frac{-\sqrt{3}B_1 + A_1 + 3D_1}{2} \right) f_{13} \\ \begin{pmatrix} 1 & 3 \\ x & y \end{pmatrix} &= B_1 f_{11} + \left(\frac{-\sqrt{3}A_1 - B_1 + D_1\sqrt{3}}{4} \right) f_{12} + \left(\frac{\sqrt{3}A_1 - B_1 - D_1\sqrt{3}}{4} \right) f_{13} \\ \begin{pmatrix} 1 & 3 \\ x & z \end{pmatrix} &= C_1 f_{11} + \left[\frac{C_1 + E_1\sqrt{3}}{2} \right] f_{12} + \left[\frac{C_1 - \sqrt{3}E_1}{2} \right] f_{13} \\ \begin{pmatrix} 1 & 3 \\ y & y \end{pmatrix} &= D_1 f_{11} + \left(\frac{-\sqrt{3}B_1 + D_1 + 3A_1}{2} \right) f_{12} + \left(\frac{\sqrt{3}B_1 + D_1 + 3A_1}{4} \right) f_{13} \\ \begin{pmatrix} 1 & 3 \\ y & z \end{pmatrix} &= -E_1 f_{11} + \left[\frac{E_1 - C_1\sqrt{3}}{2} \right] f_{12} + \left[\frac{E_1 + C_1\sqrt{3}}{2} \right] f_{13} \\ \begin{pmatrix} 1 & 3 \\ z & z \end{pmatrix} &= F_1 [f_{11} + f_{12} + f_{13}] \\ \begin{pmatrix} 1 & 4 \\ x & x \end{pmatrix} &= A_1 f_{14} + \left(\frac{A_1 + \sqrt{3}B_1 + 3D_1}{4} \right) f_{15} + \left(\frac{-\sqrt{3}B_1 - A_1 + 3D_1}{2} \right) f_{16} \\ \begin{pmatrix} 1 & 4 \\ x & y \end{pmatrix} &= B_1 f_{14} + \left(\frac{-\sqrt{3}A_1 - B_1 + D_1\sqrt{3}}{4} \right) f_{15} + \left(\frac{\sqrt{3}A_1 - B_1 - D_1\sqrt{3}}{4} \right) f_{16} \\ \begin{pmatrix} 1 & 4 \\ x & z \end{pmatrix} &= C_1 f_{14} + \left[\frac{C_1 + E_1\sqrt{3}}{2} \right] f_{15} + \left[\frac{C_1 - E_1\sqrt{3}}{2} \right] f_{16} \\ \begin{pmatrix} 1 & 4 \\ y & y \end{pmatrix} &= D_1 f_{14} + \left(\frac{-\sqrt{3}B_1 - D_1 + 3A_1}{2} \right) f_{15} + \left(\frac{\sqrt{3}B_1 + D_1 + 3A_1}{4} \right) f_{16} \\ \begin{pmatrix} 1 & 4 \\ y & z \end{pmatrix} &= -E_1 f_{14} + \left[\frac{E_1 - C_1\sqrt{3}}{2} \right] f_{15} + \left[\frac{E_1 + C_1\sqrt{3}}{2} \right] f_{16} \\ \begin{pmatrix} 1 & 4 \\ z & z \end{pmatrix} &= F_1 [f_{14} + f_{15} + f_{16}] \\ \begin{pmatrix} 2 & 5 \\ x & x \end{pmatrix} &= A_1 f_{17} + \left(\frac{A_1 + \sqrt{3}B_1 + 3D_1}{4} \right) f_{18} + \left(\frac{-\sqrt{3}B_1 + A_1 + 3D_1}{2} \right) f_{19} \\ \begin{pmatrix} 2 & 5 \\ x & y \end{pmatrix} &= B_1 f_{17} + \left(\frac{-\sqrt{3}A_1 - B_1 + D_1\sqrt{3}}{4} \right) f_{18} + \left(\frac{\sqrt{3}A_1 - B_1 - D_1\sqrt{3}}{4} \right) f_{19} \\ \begin{pmatrix} 2 & 5 \\ x & z \end{pmatrix} &= C_1 f_{17} + \left[\frac{C_1 + E_1\sqrt{3}}{2} \right] f_{18} + \left[\frac{C_1 - E_1\sqrt{3}}{2} \right] f_{19} \\ \begin{pmatrix} 2 & 5 \\ y & y \end{pmatrix} &= D_1 f_{17} + \left(\frac{-\sqrt{3}B_1 + D_1 + 3A_1}{2} \right) f_{18} + \left(\frac{\sqrt{3}B_1 + D_1 + 3A_1}{4} \right) f_{19} \\ \begin{pmatrix} 2 & 5 \\ y & z \end{pmatrix} &= E_1 f_{17} + \left[\frac{C_1\sqrt{3} - E_1}{2} \right] f_{18} + \left[\frac{C_1\sqrt{3} + E_1}{2} \right] f_{19} \\ \begin{pmatrix} 2 & 5 \\ z & z \end{pmatrix} &= F_1 [f_{17} + f_{18} + f_{19}] \\ \begin{pmatrix} 2 & 6 \\ x & x \end{pmatrix} &= A_1 f_{10} + \left(\frac{A_1 + \sqrt{3}B_1 + 3D_1}{2} \right) f_{111} + \left(\frac{-\sqrt{3}B_1 - A_1 - 3D_1}{4} \right) f_{112} \\ \begin{pmatrix} 2 & 6 \\ x & y \end{pmatrix} &= B_1 f_{10} + \left(\frac{-\sqrt{3}A_1 - B_1 + D_1\sqrt{3}}{4} \right) f_{111} + \left(\frac{\sqrt{3}A_1 - B_1 - D_1\sqrt{3}}{4} \right) f_{112} \\ \begin{pmatrix} 2 & 6 \\ x & z \end{pmatrix} &= C_1 f_{10} + \left[\frac{C_1 + E_1\sqrt{3}}{2} \right] f_{111} + \left[\frac{-C_1 + E_1\sqrt{3}}{2} \right] f_{112} \\ \begin{pmatrix} 2 & 6 \\ y & y \end{pmatrix} &= D_1 f_{10} + \left(\frac{-\sqrt{3}B_1 + D_1 + 3A_1}{2} \right) f_{111} + \left(\frac{\sqrt{3}B_1 + D_1 + 3A_1}{4} \right) f_{112} \\ \begin{pmatrix} 2 & 6 \\ y & z \end{pmatrix} &= E_1 f_{10} + \left[\frac{C_1\sqrt{3} - E_1}{2} \right] f_{111} + \left[\frac{C_1\sqrt{3} + E_1}{2} \right] f_{112} \\ \begin{pmatrix} 2 & 6 \\ z & z \end{pmatrix} &= F_1 [f_{10} + f_{111} + f_{112}] \\ \begin{pmatrix} 3 & 3 \\ x & x \end{pmatrix} &= 2A_2 h_1 \left[\left(\frac{a^2}{9\Gamma^2} \right) h_{11} + (1 + 2\sqrt{3}) \left(\frac{a^2}{36\Gamma^2} \right) h_{12} + (1 - 2\sqrt{3}) \left(\frac{a^2}{36\Gamma^2} \right) h_{13} \right] \end{aligned}$$

$$\begin{pmatrix} 5 & 6 \\ x & x \end{pmatrix} = 6B_5 f_9$$

$$\begin{pmatrix} 5 & 6 \\ y & y \end{pmatrix} = 6B_5 f_6$$

$$\begin{pmatrix} 3 & 4 \\ z & z \end{pmatrix} = 6f_9 \left[(A_3 \cdot B_3) \left(2u + \frac{1}{2} \right)^2 \frac{c^2}{r^2} + B_5 \right]$$

Where:

$$f_1 = \exp\left(\frac{-i\pi u Q_3}{2}\right)$$

$$f_2 = \exp(i\pi u Q_3)$$

$$f_3 = \exp\left(\frac{i\pi u Q_3}{2}\right)$$

$$f_4 = \exp\left(2\pi i \left((5u-2) \frac{Q_3}{4} - 0.3849 Q_1 - 0.859116 Q_2 \right)\right)$$

$$f_{12} = \exp\left(2\pi i \left((5u-2) \frac{Q_3}{4} - 0.474216 Q_1 + 0.3849 Q_2 \right)\right)$$

$$f_{13} = \exp\left(2\pi i \left((5u-2) \frac{Q_3}{4} + 0.85911 Q_1 + 0.47421 Q_2 \right)\right)$$

$$f_{14} = \exp\left(2\pi i \left(\left(\frac{-3uQ_3}{4} \right) - 0.3849 Q_1 + 0.859116 Q_2 \right)\right)$$

$$f_{15} = \exp\left(2\pi i \left(\left(\frac{-3uQ_3}{4} \right) - 0.474216 Q_1 + 0.474216 Q_2 \right)\right)$$

$$f_{17} = \exp\left(2\pi i \left(\frac{3uQ_3}{4} + 0.3849 Q_1 + 0.859116 Q_2 \right)\right)$$

$$f_{18} = \exp\left(2\pi i \left(\frac{3uQ_3}{4} + 0.3849 Q_1 + 0.859116 Q_2 \right)\right)$$

$$f_{19} = \exp\left(2\pi i \left(\frac{3uQ_3}{4} - 0.859116 Q_1 - 0.474216 Q_2 \right)\right)$$

$$f_{10} = \exp\left(2\pi i \left(-(5u+2) \left(\frac{Q_3}{4} \right) + 0.3849 Q_1 + 0.859116 Q_2 \right)\right)$$

$$f_{112} = \exp\left(2\pi i \left(-(5u+2) \left(\frac{Q_3}{4} \right) - 0.859116 Q_1 - 0.474216 Q_2 \right)\right)$$

$$h_1 = \cos\left(2\pi Q_3 \left(\frac{u-1}{2} \right)\right) + i \sin\left(2\pi Q_3 \left(\frac{u-1}{2} \right)\right)$$

$$h_2 = -\sin\left(2\pi Q_3 \left(\frac{u-1}{2} \right)\right) + i \cos\left(2\pi Q_3 \left(\frac{u-1}{2} \right)\right)$$

$$h_3 = \cos\left(2\pi u Q_3 \left(\frac{u-1}{2} \right)\right) - i \sin(2\pi u Q_3)$$

$$h_4 = \sin(2\pi u Q_3) + i \cos(2\pi u Q_3)$$

$$h_5 = \cos(2\pi u Q_3) + i \sin(2\pi u Q_3)$$

$$h_6 = \sin(2\pi u Q_3) - i \cos(2\pi u Q_3)$$

$$h_7 = \cos\left(2\pi Q_3 \left(\frac{u+1}{2} \right)\right) - i \sin\left(2\pi Q_3 \left(\frac{u+1}{2} \right)\right)$$

$$h_8 = \cos\left(2\pi Q_3 \left(\frac{u+1}{2} \right)\right) + i \cos\left(2\pi Q_3 \left(\frac{u+1}{2} \right)\right)$$

$$h_{11} = \cos(2\pi(0.3849 Q_1 + 0.859116 Q_2))$$

$$h_{12} = \cos(2\pi(0.859116 Q_1 + 0.474216 Q_2))$$

$$h_{13} = \cos(2\pi(0.474216 Q_1 - 0.3849 Q_2))$$

$$g_{11} = \sin(2\pi(0.3849 Q_1 + 0.859116 Q_2))$$

$$g_{12} = \sin(2\pi(0.859116 Q_1 + 0.474216 Q_2))$$

$$g_{13} = \sin(2\pi(0.474216 Q_1 - 0.3849 Q_2))$$

where, Q_1 , Q_2 and Q_3 are the phonon wave vector components along b_1 , b_2 and b_3 . Fig. 1: Phonon frequency distribution.

REFERENCES

- Balaguru, R.J.B., N. Lawrence and S.A.C. Raj, 2002. Lattice Instability of 2H-TaSe₂. *Int. J. Mod. Phys. B*, 16: 4111-4125.
- Berman, R., 1976. *Thermal Conduction in Solids*. Clarendon Press, Oxford, UK., ISBN-13: 978-0198514299, Pages: 206.
- Brouet, V., W.L. Yang, X.J. Zhou, Z. Hussain and N. Ru *et al.*, 2004. Fermi surface reconstruction in the CDW state of CeTe₃ observed by photoemission. *Phys. Rev. Lett.*, Vol. 93. 10.1103/PhysRevLett.93.126405
- Craven, R.A. and S.F. Meyer, 1977. Specific heat and resistivity near the charge-density-wave phase transitions in 2H-TaSe₂ and 2H-TaS₂. *Phys. Rev. B*, 16: 4583-4593.
- Di Salvo, F.J., D.E. Moncton and J.V. Waszczak, 1976. Electronic properties and superlattice formation in the semimetal TiSe₂. *Phys. Rev. B*, 14: 4321-4328.

- Frohlich, H., 1954. On the theory of superconductivity: The one-dimensional case. Proc. R. Soc. London Ser. A. Math. Phys. Sci., 223: 296-305.
- Harper, J.M.E., T.H. Geballe and F.J. DiSalvo, 1977. Thermal properties of layered transition-metal dichalcogenides at charge-density-wave transitions. Phys. Rev. B, 15: 2943-2951.
- Lavagnini, M., A. Sacchetti, L. Degiorgi, E. Arcangeletti and L. Baldassarre *et al.*, 2008. Pressure dependence of the optical properties of the charge-density-wave compound LaTe_2 . Phys. Rev. B, Vol. 77. 10.1103/PhysRevB.77.165132
- Maradudin, A.A., E.W. Montroll, C.H. Weiss and I.P. Ipatova, 1971. Theory of Lattice Dynamics in the Harmonic Approximation. 2nd Edn., Academic Press, New York, Pages: 708.
- Moncton, D.E., J.D. Axe and F.J. DiSalvo, 1977. Neutron scattering study of the charge-density wave transitions in 2H-TaSe_2 and 2H-NbSe_2 . Phys. Rev. B, 16: 801-819.
- Nunez-Regueiro, M.D., J.M. Lopez-Castillo and C. Ayache, 1985. Thermal conductivity of 1T-TaS_2 and 2H-TaSe_2 . Phys. Rev. Lett., 55: 1931-1934.
- Peierls, R.E., 1995. Quantum Theory of Solids. Oxford University Press, Oxford, Pages: 108.
- Rinaldi, R.P. and G.S. Pawley, 1975. An investigation of the intermolecular modes in orthorhombic sulphur. J. Phys. C: Solid State Phys., 8: 599-616.
- Shin, K.Y., V. Brouet, N. Ru, Z.X. Shen and I.R. Fisher, 2005. Electronic structure and charge-density wave formation in $\text{LaTe}_{1.95}$ and $\text{CeTe}_{2.00}$. Phys. Rev. B, Vol. 72. 10.1103/PhysRevB.72.085132
- Smith, T.F., R.N. Shelton and R.E. Schwall, 1975. Superconductivity of $\text{TaS}_{2-x}\text{Se}_x$ layer compounds at high pressure. J. Phys. F: Metal Phys., 5: 1713-1725.
- Sugai, S., 1985. Lattice vibrations in the charge-density-wave states of layered transition metal dichalcogenides. Phys. Status Solidi (B), 129: 13-39.
- Sugai, S., K. Murase, S. Uchida and S. Tanaka, 1981. Studies of lattice dynamics in 2H-TaS_2 by Raman scattering. Solid State Commun., 40: 399-401.
- Wilson, J.A., F.J. Di Salvo and S. Mahajan, 2001. Charge-density waves and superlattices in the metallic layered transition metal dichalcogenides. Adv. Phys., 50: 1171-1248.